Geophysical Journal International

Geophys. J. Int. (2016) **206,** 999–1008
Advance Access publication 2016 May 12
GJI Gravity, geodesy and tides

doi: 10.1093/gji/ggw182

Rotation change in the orientation of the centre-of-figure frame caused by large earthquakes

Jiangcun Zhou,[1] Wenke Sun,[2] Shuanggen Jin,[3] Heping Sun[1] and Jianqiao Xu[1]

[1] *State Key Laboratory of Geodesy and Earth's Dynamics, Institute of Geodesy and Geophysics, Chinese Academy of Sciences, Wuhan* 430077, *China.*
E-mail: zjc@asch.whigg.ac.cn
[2] *Key Laboratory of Computational Geodynamics, University of Chinese Academy of Sciences, Beijing* 100049, *China*
[3] *Key Laboratory of Planetary Sciences, Shanghai Astronomical Observatory, Chinese Academy of Science, Shanghai* 200030, *China*

Accepted 2016 May 10. Received 2016 May 7; in original form 2015 July 30

SUMMARY

A method to estimate the rotation change in the orientation of the centre-of-figure (CF) frame caused by earthquakes is proposed for the first time. This method involves using the point dislocation theory based on a spherical, non-rotating, perfectly elastic and isotropic (SNREI) Earth. The rotation change in the orientation is related solely to the toroidal displacements of degree one induced by the vertical dip slip dislocation, and the spheroidal displacements induced by an earthquake have no contribution. The effects of two recent large earthquakes, the 2004 Sumatra and the 2011 Tohoku-Oki, are studied. Results showed that the Sumatra and Tohoku-Oki earthquakes both caused the CF frame to rotate by at least tens of μas (micro-arc-second). Although the visible co-seismic displacements are identified and removed from the coordinate time-series, the rotation change due to the unidentified ones and errors in removal is non-negligible. Therefore, the rotation change in the orientation of the CF frame due to seismic deformation should be taken into account in the future in reference frame and geodesy applications.

Key words: Numerical solutions; Reference systems; Space geodetic surveys; Earthquake ground motions.

1 INTRODUCTION

Earth-related frames are usually defined as centre of mass of the whole Earth (CM), centre of mass of the solid Earth (CE) and centre of figure of the outer surface of the solid Earth (CF) frames, whose origins are correspondingly located at CM, CE and CF and whose orientations are arbitrarily or conventionally defined (Dong *et al.* 1997; Blewitt 2003; IERS Conventions 2010; Wu *et al.* 2012; Zhang & Jin 2014). When there are no external net forces acting on the Earth system, the linear and angular momentums of the whole Earth are conserved (Ben-Menahem & Singh 1968). The mechanism of an earthquake can be represented by a double couple, which is an internal force within the whole Earth system. In this way, the CM frame does not change after an earthquake. However the CF frame is only defined by the outer surface of the solid Earth, which is not conserved in the linear and angular momentums, so it may change after an earthquake.

The CF frame is currently widely used in geodesy because tracking stations with high-precision geodetic techniques, such as GPS and VLBI, are used on the Earth's surface (Jin & Park 2006). With the improvement of the observation accuracy, CF and CM frames can now be distinguished from one another (Dong *et al.* 2003). For this reason, many studies have been conducted on the seasonal and secular geocentral movement caused by the redistribution of the fluid envelope, including the atmosphere, ocean and land water (Jin *et al.* 2011), in which the geocentral movement is defined as any change in CF relative to CM or vice versa (Dong *et al.* 1997; Chen *et al.* 1999; Collilieux *et al.* 2010; Métivier *et al.* 2010; Jin *et al.* 2013). Colilieux *et al.* (2010) showed that the rotation parameters were not significantly different from zero when they considered the loading impact. This may be because the loading induces only spheroidal displacements, which do not cause the CF frame to rotate.

For the co-seismic effect on CF frame, Zhou *et al.* (2015) investigated the co-seismic change of CF relative to CM due to the 2004 Sumatra ($M_w = 9.3$) and 2011 Tohoku-Oki ($M_w = 9.0$) earthquakes that caused CF to move by about 4 and 2 mm, respectively. These magnitudes are observable at present using high-precision geodesy, for example, GPS. However the rotation of the CF frame due to earthquakes is still an open question, and it may affect the construction of the terrestrial reference frame (e.g. ITRF). So far, most previous works related to CF frame were focused on the origin change of the CF frame relative to the CM frame, that is, motion of the geocentre, caused by loading effects (e.g. Dong *et al.* 1997, 2014; Chen *et al.* 1999), while no one knows the rotation change of the CF frame caused by earthquakes. From the spherical geometry, a rotation of 1 mas (milli-arc-second) corresponds to 30 mm on the Earth's surface. The present GPS can determine position with mm

or submillimetre precision. Therefore a rotation of several μas or larger is worth taking into account.

In this paper, the possible rotation of the CF frame due to earthquake was investigated using the point dislocation theory based on the spherical, non-rotating, perfectly elastic and isotropic (SNREI) Earth model developed by Sun (1992). Zhou *et al.* (2015) showed that the translation of the CF frame is related solely to the spheroidal co-seismic displacements of degree one. An earthquake causes not only spheroidal but also toroidal displacements. We will show that the rotation of the CF frame is only related to the toroidal co-seismic displacements, also of degree one. The toroidal degree one solution is specific because it has an analytical form, so no numerical integration is needed (Sun *et al.* 1996; Sun & Dong 2014). However, Sun *et al.* (1996) and Sun & Dong (2014) actually gave the solution for a homogeneous Earth, consistent with findings reported by Ben-Menahem & Singh (1968). Consequently, the stratified distribution of density of the SNREI Earth model was added to give a realistic solution.

2 CO-SEISMIC ROTATION OF CF FRAME

Conservation of the linear and angular momentums of the Earth can be represented, respectively, by volume integrals

$$\iiint_V \rho(r)\boldsymbol{u}\,\mathrm{d}V = 0 \tag{1}$$

and

$$\iiint_V \rho(r)\boldsymbol{r}\times\boldsymbol{u}\,\mathrm{d}V = 0 \tag{2}$$

Here, ρ is the density of the Earth, V is the Earth's volume, $\boldsymbol{r}$ is a vector denoting the location of any point in the Earth and $\boldsymbol{u}$ is a vector denoting the displacements in the Earth. Ben-Menahem & Singh (1968) gave the same two equations except they considered a homogeneous Earth and hence dropped density. For the stratified Earth assumed here, however, the density cannot be dropped. Eq. (1) is for conserving the centre of mass, which was used for co-seismic geocentre motion (Zhou *et al.* 2015).

Actually, eq. (2) is the definite integral of the angular momentum with respect to time, that is, $\boldsymbol{u} = \int_0^\tau \boldsymbol{v}\mathrm{d}t$, where τ is the duration of an earthquake and $\boldsymbol{v}$ is the velocity of the earth's particle (Chao 2015, personal communication). In dislocation theory, eqs (1) and (2) are used as two additional boundary conditions to solve the spheroidal and toroidal solutions, respectively, of degree one (Sun 1992; Okubo 1993; Sun *et al.* 1996). In this way, earthquakes cause no net translation or rotation in the CM frame.

However, considering only Earth's surface according to eq. (2), that is, the volume integral degenerating to an area integral, the rotation of CF frame can be presented in the first order approximation as followings:

$$\boldsymbol{R} = \frac{1}{I}\iint_S \boldsymbol{r}\times\boldsymbol{u}\mathrm{d}S \tag{3}$$

where $\boldsymbol{R}$ is a vector including three independent elements of the antisymmetric rotation matrix, $I = 8\pi a^4/3$ is the polar moment of inertia of the Earth's surface (with unit surface density), a is the radius of the Earth, S is Earth's entire surface, and $\boldsymbol{r}$ and $\boldsymbol{u}$ are on the Earth's surface rather than beneath it. The Lagrangian description is implicitly adopted in eq. (3). The moment of inertia, including I, of the whole Earth is slightly changed after an earthquake, which is due to co-seismic spheroidal deformation of degree two (Zhou *et al.* 2013). The co-seismic change of I is here ignored because when it is multiplied by $\boldsymbol{u}$ it causes a negligible one-order smaller effect.

In Cartesian coordinate system, the three components of $\boldsymbol{u}$ are expressed as followings:

$$\left.\begin{aligned} u_X(\theta,\varphi) &= u_r\sin\theta\cos\varphi + u_\theta\cos\theta\cos\varphi - u_\varphi\sin\varphi \\ u_Y(\theta,\varphi) &= u_r\sin\theta\sin\varphi + u_\theta\cos\theta\sin\varphi + u_\varphi\cos\varphi \\ u_Z(\theta,\varphi) &= u_r\cos\theta - u_\theta\sin\theta \end{aligned}\right\}. \tag{4}$$

Here, u_r, u_θ and u_ϕ are the three components of $\boldsymbol{u}$ in the spherical coordinate system and are also dependent on co-latitude θ and longitude ϕ. Here, $\boldsymbol{r}$ can be represented in the Cartesian coordinate system as follows:

$$\boldsymbol{r} = \begin{pmatrix} X \\ Y \\ Z \end{pmatrix} = \begin{pmatrix} a\sin\theta\cos\varphi \\ a\sin\theta\sin\varphi \\ a\cos\theta \end{pmatrix}. \tag{5}$$

Substituting eqs (4) and (5) into eq. (3) shows the following to be true:

$$\begin{aligned} \boldsymbol{R} &= \begin{pmatrix} R_X \\ R_Y \\ R_Z \end{pmatrix} \\ &= \frac{3}{8\pi a}\int_0^{2\pi}\int_0^{\pi}\begin{pmatrix} -u_\theta\sin\varphi - u_\varphi\cos\theta\cos\varphi \\ u_\theta\cos\varphi - u_\varphi\cos\theta\sin\varphi \\ u_\varphi\sin\theta \end{pmatrix}\sin\theta\,\mathrm{d}\theta\,\mathrm{d}\varphi. \end{aligned} \tag{6}$$

This is related to horizontal displacements only. The kernel of the integral, that is, dependences on the co-latitude and longitude in parenthesis, shows that only degree one displacements contribute to the integral due to the orthogonality of the spherical harmonics.

If the rotation is determined by a network, the integral is changed to a summation of all the stations in the network, that is,

$$\boldsymbol{R} = \frac{3}{2a}\frac{\sum_{i=1}^{N}\boldsymbol{K}_i}{N}. \tag{7}$$

Here, $\boldsymbol{K}$ is the kernel of the integral in eq. (6), also a vector consisting of x, y and z components, and N is the number of the stations in the network, i is station index.

As a consequence, the coordinates in CM and CF frames can be transformed by each other through a rotation, as shown below:

$$\begin{pmatrix} X \\ Y \\ Z \end{pmatrix}_{\mathrm{CM}} = \begin{pmatrix} 0 & -R_Z & R_Y \\ R_Z & 0 & -R_X \\ -R_Y & R_X & 0 \end{pmatrix}\begin{pmatrix} X \\ Y \\ Z \end{pmatrix}_{\mathrm{CF}} \tag{8}$$

Alternatively, we can link the coordinates before and after earthquake by

$$\begin{aligned} &\begin{pmatrix} X \\ Y \\ Z \end{pmatrix}_{\mathrm{after}} - \begin{pmatrix} X \\ Y \\ Z \end{pmatrix}_{\mathrm{before}} \\ &= \boldsymbol{b} = \begin{pmatrix} 1 & 0 & 0 & X & 0 & -Z & Y \\ 0 & 1 & 0 & Y & Z & 0 & -X \\ 0 & 0 & 1 & Z & -Y & X & 0 \end{pmatrix}_{\mathrm{before}}\begin{pmatrix} T_X \\ T_Y \\ T_Z \\ D \\ R_X \\ R_Y \\ R_Z \end{pmatrix} = \boldsymbol{A}\boldsymbol{x} \end{aligned} \tag{9}$$

The unknown $\boldsymbol{x}$, containing translation (T_X, T_Y, T_Z), scale factor D and rotation (R_X, R_Y, R_Z), can be solved by least-squares method

provided sufficient stations are involved. The equally weighted solution is

$$\boldsymbol{x} = (\boldsymbol{A}^T\boldsymbol{A})^{-1}\boldsymbol{A}^T\boldsymbol{b} \tag{10}$$

If the stations distribute densely everywhere on the Earth's surface, the rotation derived from eq. (10) will be identical to that from eq. (3). To show this, one can represent the station number N mathematically by

$$N = \frac{4\pi a^2}{\sin\theta \mathrm{d}\theta \mathrm{d}\lambda}. \tag{11}$$

As a consequence, the summation in eq. (10) becomes integral and the matrix $\boldsymbol{A}^T\boldsymbol{A}$ is diagonal due to the orthogonality of the spherical harmonics. The derivation is straightforward. Hereafter, we call eq. (7) summation method and eq. (10) transformation method.

Similarly to Zhou *et al.* (2015), the epicentre was first located at the North Pole (NP). The degree one horizontal displacements then have the following form:

$$\left.\begin{aligned} u_\theta^{31} &= 2y_3^{31}\cos\theta\cos\varphi \\ u_\theta^{32} &= 2y_3^{32}\cos\theta\sin\varphi \\ u_\theta^{22,0} &= -y_3^{22,0}\sin\theta \\ u_\theta^{33} &= -y_3^{33}\sin\theta \end{aligned}\right\} \tag{12a}$$

$$\left.\begin{aligned} u_\varphi^{31} &= -2y_3^{31}\sin\varphi \\ u_\varphi^{32} &= 2y_3^{32}\cos\varphi \\ u_\varphi^{22,0} &= 0 \\ u_\varphi^{33} &= 0 \end{aligned}\right\} \tag{12b}$$

for spheroidal solutions and

$$\left.\begin{aligned} u_\theta^{31,t} &= 2y_{1,t}^{31}\cos\varphi \\ u_\theta^{32,t} &= 2y_{1,t}^{32}\sin\varphi \\ u_\varphi^{31,t} &= -2y_{1,t}^{31}\cos\theta\sin\varphi \\ u_\varphi^{32,t} &= 2y_{1,t}^{32}\cos\theta\cos\varphi \end{aligned}\right\} \tag{12c}$$

for toroidal solutions. The variables y_3 and $y_{1,t}$ denote the spheroidal and toroidal horizontal displacements, respectively. These are used to define the dislocation Love number. The superscript numbers indicate the independent fault types (Sun 1992; Sun *et al.* 1996). The vertical strike-slip (superscript number 12) has no degree one solution.

Substituting eqs (12a), (12b) and (12c) into eq. (6) and applying the orthogonal properties of the spherical harmonics shows that the vertical dip slip dislocation (superscripts 31 and 32) is the only thing that contributes to the rotation. For any other types of dislocation, the integral of eq. (6) is zero. For vertically tensile fault, the following example is given:

$$\begin{aligned} R_X^{33} &= \frac{3}{8\pi a}\int_0^{2\pi}\int_0^{\pi}\left(-u_\theta^{33}\sin\varphi - u_\varphi^{33}\cos\theta\cos\varphi\right)\sin\theta \mathrm{d}\theta \mathrm{d}\varphi \\ &= \frac{3}{8\pi a}\int_0^{2\pi}\int_0^{\pi}\left(y_3^{33}\sin\theta\sin\varphi - 0\right)\sin\theta \mathrm{d}\theta \mathrm{d}\varphi \\ &= \frac{3}{8\pi a}\int_0^{\pi}\left(y_3^{33}\sin\theta\right)\sin\theta \mathrm{d}\theta \int_0^{2\pi}\sin\varphi \mathrm{d}\varphi \\ &= 0 \end{aligned} \tag{13}$$

Similarly, the R_Y^{33} and R_Z^{33} and those of horizontally tensile dislocation (superscript 22,0) are all zero. Finally, with the same procedures in eq. (13), the non-zero elements of the rotation matrix are as follows:

$$\left.\begin{aligned} R_x^{32} &= -2y_{1,t}^{32}/a \\ R_y^{31} &= 2y_{1,t}^{31}/a \end{aligned}\right\}. \tag{14}$$

Eq. (14) shows that only the toroidal displacement due to vertical dip slip contributes to the rotation of CF frame.

If the dip angle (δ) and slip angle (λ) are both taken into account, the rotation vector for epicentre at NP is consequently (Sun & Okubo 1993)

$$\boldsymbol{R}_{\mathrm{NP}} = \begin{pmatrix} R_X \\ R_Y \\ R_Z \end{pmatrix} = \begin{pmatrix} R_x^{32}\sin\lambda\cos 2\delta \\ R_y^{31}\cos\lambda\cos\delta \\ 0 \end{pmatrix} \tag{15a}$$

for a shear dislocation and

$$\boldsymbol{R}_{\mathrm{NP}} = \begin{pmatrix} R_X \\ R_Y \\ R_Z \end{pmatrix} = \begin{pmatrix} -R_x^{32}\sin 2\delta \\ 0 \\ 0 \end{pmatrix} \tag{15b}$$

for a tensile dislocation.

For the epicentre at an arbitrary position, the rotation vector is as follows:

$$\boldsymbol{R} = \boldsymbol{r}_{\mathrm{rot}}(-\varphi_0)\boldsymbol{\varphi}_{\mathrm{rot}}(-\theta_0)\boldsymbol{r}_{\mathrm{rot}}(-\pi+\alpha)\boldsymbol{R}_{\mathrm{NP}} \tag{16}$$

Here, α is the strike angle, θ_0 and ϕ_0 are the respective co-latitude and longitude of the epicentre, and $\boldsymbol{r}_{\mathrm{rot}}$ and $\boldsymbol{\varphi}_{\mathrm{rot}}$ represent the rotation matrix in the following forms

$$\mathbf{r}_{\mathrm{rot}}(\beta) = \begin{pmatrix} 1 & 0 & 0 \\ 0 & \cos\beta & \sin\beta \\ 0 & -\sin\beta & \cos\beta \end{pmatrix},$$

$$\boldsymbol{\varphi}_{\mathrm{rot}}(\beta) = \begin{pmatrix} \cos\beta & \sin\beta & 0 \\ -\sin\beta & \cos\beta & 0 \\ 0 & 0 & 1 \end{pmatrix}. \tag{17}$$

3 RESULTS AND DISCUSSIONS

3.1 Toroidal displacements of degree one

The $y_{1,t}$ values on the Earth's surface were first computed for different hypocentres using the theory in Appendix A and the PREM model (Dziewonski & Anderson 1981). Values with superscripts of 31 and 32 are theoretically identical. The results are shown in Fig. 1. The deeper the earthquake is, the smaller the co-seismic toroidal displacement of degree one on the Earth's surface is. The magnitude decreases nearly linearly and smoothly from 1.47×10^{-15} to 1.23×10^{-15} with respect to the depth of the hypocentre. As we know, only large earthquakes cause significant co-seismic effects and large earthquakes usually have shallow hypocentres, so an approximate value of about 1.465×10^{-15} of $y_{1,t}$ can be used for convenient computation although $y_{1,t}$ has an exact value.

3.2 CF frame rotation

Computation theory was used on the 2004 Sumatra and the 2011 Tohoku-Oki earthquakes in order to numerically estimate to what extent large earthquakes cause the CF frame to rotate. Because of their large magnitudes, these two earthquakes cannot be considered point sources (Sun & Okubo 1998). Therefore finite fault models ought to be used. Three finite fault models of the 2004 Sumatra

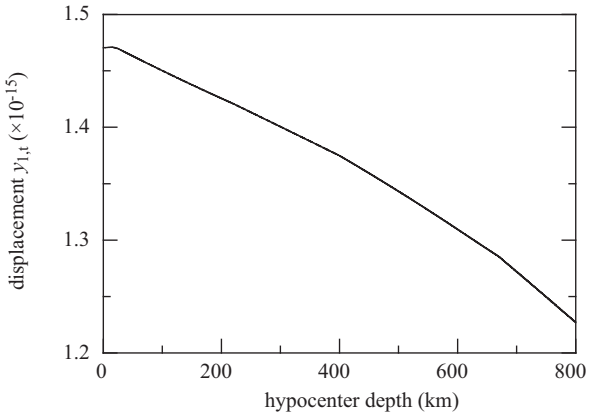

Figure 1. Toroidal displacements of degree one on the Earth's surface due to vertical dip slips for different hypocentre depths.

earthquake were used. They are denoted as Chlieh (Chlieh *et al.* 2007), USGS (Ji 2004) and USGS-Ji (Han *et al.* 2006). Three finite fault models of 2011 Tohoku-Oki earthquake were also used. They are denoted as USGS (Hayes 2011), ARIA (Wei *et al.* 2011) and UCSB (Shao *et al.* 2011). The results for all finite fault models are listed in Table 1.

For the 2014 Sumatra earthquake, the results from different finite fault models were quite different. The magnitudes of the rotation vectors computed by the three finite fault models were 92.8, 47.0 and 200.3 μas, respectively. Generally speaking, larger earthquake moments produce rotation vectors with larger magnitudes. However, the three components of the rotation vectors are highly dependent on the details of the fault parameters such as the strike, dip and rake angles. Fig. 2 shows intuitively how each subfault of the fault models contributes to the final rotation vectors after scaling with their moments, that is, the values of the three models are divided by 6.68, 2.57 and 9.65, respectively, from which one can see detail contributions from all sub-faults and the overall features of the differences between the fault models. It is noted that the fault area of the USGS model is much smaller compared with the other two models.

The three sets of results regarding the directions of the rotations, that is, clockwise or counter-clockwise, remained relatively consistent along the three axes. The values produced by the USGS-Ji model were −45.4, 4.5 and −195.0 μas for R_x, R_y and R_z, respectively. This means that the CF frame rotated clockwise by 45.4 μas along X axis, then 195.0 μas along Z axis, and then counter-clockwise by 4.5 μas along the Y axis. Because the angles rotated are very small, the order of rotation along the axes was negligible. This earthquake caused the CF frame to rotate significantly along the Z and visibly but not significantly along the Y axis. To intuitively inspect the consistency of the orientation changes computed from the three fault models, we plot the locations of Euler poles of the rotations computed from the three fault models with purple stars in Fig. 3. The poles obtained from Chlieh and USGS-Ji models are close while they are much far away from that computed from USGS model.

For the 2011 Tohoku-Oki earthquake, the results computed from three finite fault models showed a good consistency. Here, the values of R_x and R_z have minus signs while those of R_y have plus signs, as for the 2004 Sumatra earthquake. This earthquake caused the CF frame to rotate significantly along all the three axes simultaneously. Numbers produced from different finite fault models for three components of the rotation vectors would all be similar to each other if the earthquake moments were taken into account. Identically, the Euler poles are plotted with blue stars in Fig. 3. One can find the consistency among them, especially between those obtained from USGS and UCSB models. Fig. 4 shows how each sub-fault contributes to the final rotation vectors after scaling with their moments. Similarly, the values of the three models are divided by 4.37, 5.53 and 4.74 respectively. One can clearly see the differences among the results from different fault models, such as the locations where the extremes appear.

The results obtained by setting the $y_{1,t}$ value to be 1.465×10^{-15} are also given in Table 1. They showed the values to be nearly identical to those obtained using the true $y_{1,t}$ values. This shows that the approximation is valid and the approximate value of 1.465×10^{-15} is applicable for the future computations.

3.3 Network effect

To evaluate the network effect in estimating the rotation of CF frame using geodetic techniques such as GPS, the rotation parameters of the CF frame were first computed for the same two large earthquakes as above. However, point sources rather than finite fault models of these earthquakes were used for simplicity. The result from a finite model was the sum of result of each sub-fault which was considered a point source. In this way, the results from the point source are still instructive. The mechanisms of these two earthquakes were from the global CMT solution (www.globalcmt.org). Using the same computation theory, the rotation parameters of the CF frame, considered as the theoretical result, were determined and are listed in Table 2.

The co-seismic displacements, including spheroidal and toroidal ones of all degrees, at the 937 geodetic stations (Fig. 3) were computed using the theory reported by Sun *et al.* (1996). It is here supposed that these co-seismic displacements are observed at these stations. The reason why these stations were used is that the geodetic observations conducted by GPS, BLVI, DORIS and SLR techniques at these stations are used to construct the ITRF (Altamimi *et al.* 2011). Co-seismic displacements were used to compute the rotation of the CF frame using eqs (7) and (10), respectively. The results are given in parentheses in Table 2.

Table 1. Rotation of CF frame due to Co-seismic displacements.

	2004 Sumatra earthquake			2011 Tohoku-Oki earthquake		
	Chlieh	USGS	USGS-Ji	USGS	ARIA	UCSB
Moment (10^{22} N m)	6.68	2.57	9.65	4.37	5.53	4.74
Rx (μas)	−27.7/−27.6	−3.8/−3.8	−45.4/−45.2	−53.6/−53.5	−61.9/−61.7	−73.3/−73.1
Ry (μas)	1.0/1.0	3.1/3.1	4.5/4.5	44.5/44.4	70.0/69.6	61.9/61.6
Rz (μas)	−88.6/−88.4	−46.7/−46.6	−195.0/−194.3	−31.1/−31.0	−55.3/−55.1	−42.2/−42.0
$\|\boldsymbol{R}\|$ (μas)	92.8/92.6	47.0/46.9	200.3/200.0	76.3/76.1	108.6/108.1	104.8/104.4

Note: Moments are computed by elastic modulus of the PREM earth model and the dislocations of all the sub-faults. Values before slash are computed with true $y_{1,t}$ while the ones after the slash are computed with $y_{1,t} = 1.465 \times 10^{-15}$.

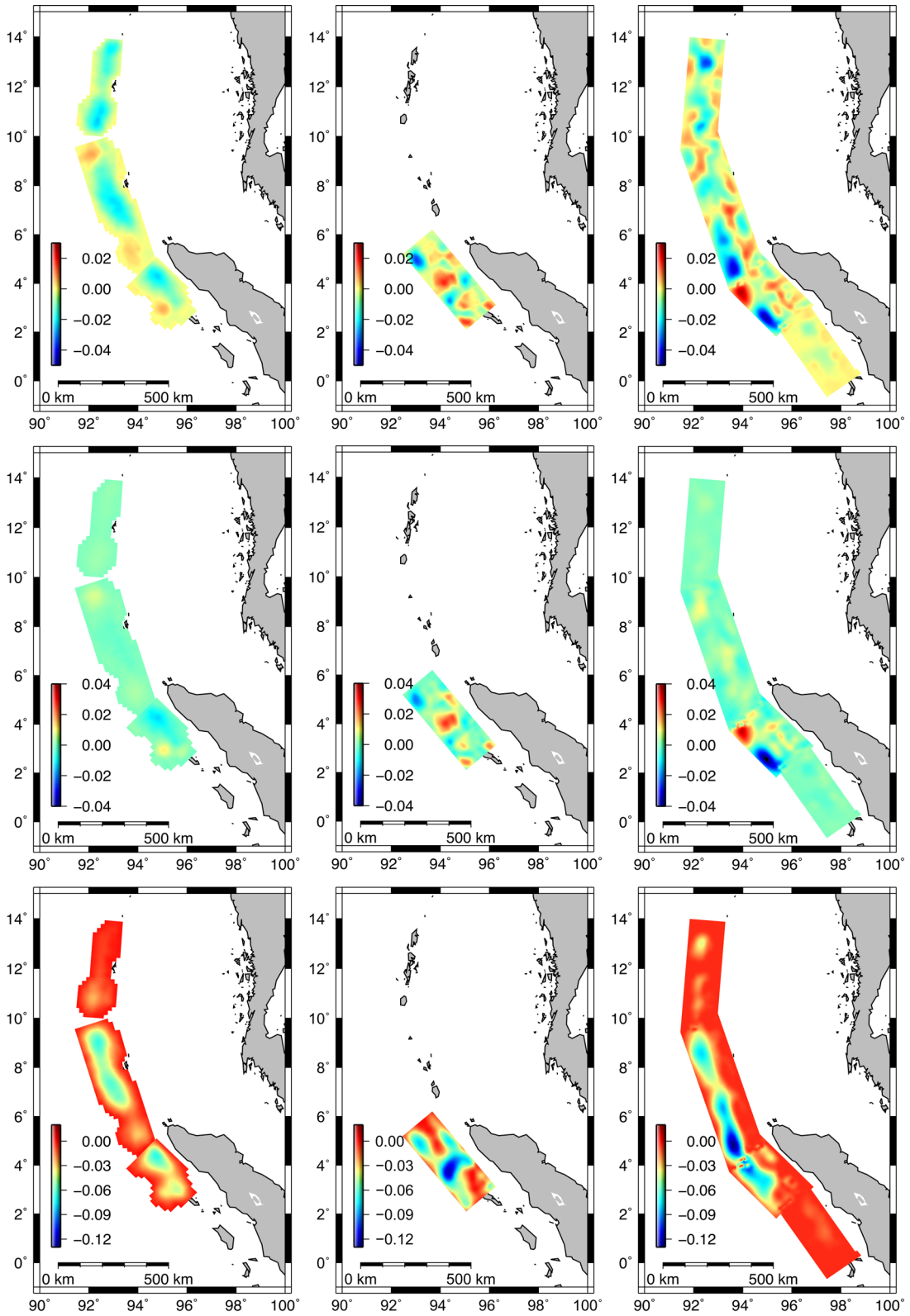

Figure 2. Contribution of each subfault to the rotation change of CF frame for three fault models of Sumatra earthquake. These results are for Chlieh, USGS and USGS-Ji models, respectively, from left to right, and for X, Y and Z components, respectively, from top to bottom. The results are scaled with the corresponding seismic scalar moments.

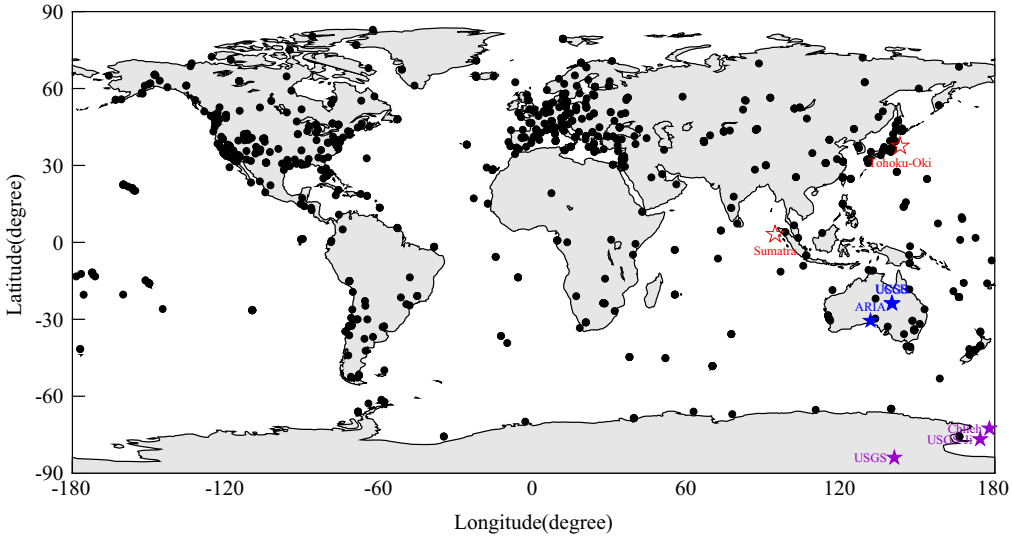

Figure 3. Distribution of the geodetic stations (dots) and the epicentres of the recent two large earthquakes (hollow stars) as well as the Euler poles computed from different fault models of these two earthquakes (purple stars for Sumatra and blue stars for Tohoku-Oki).

The results computed in terms of the co-seismic displacements at the geodetic stations by summation method are quite different from the theoretical ones, which show large network effect. For the Sumatra earthquake, the results from geodetic observations were much smaller than those from point dislocation theory. However, they were closely consistent regarding the directions of rotation of the CF frame. As shown in Fig. 3, few stations are located around the epicentre in the near-field, which may be why the magnitude of the rotation inferred from geodetic observations is smaller than that predicted by theory because large deformation occurs in the near-field and deformation decreases rapidly in the far-field. For this reason, the lack of sufficient stations in the near-field led to insufficient co-seismic deformation observed in the summation of eq. (7). Fig. 5 shows the summation changing with the epicentric distance. It shows that the co-seismic displacements in the far-field (about 150°) still have large contributions to the summation. This is due to the lack of stations in the near-field, which makes the co-seismic displacements in the far-field not be much smaller compared with the co-seismic displacements in the area which is relatively closer to the epicentre. In fact, including the long distant stations in the far-field will decrease the rotation vector in eq. (7) because the co-seismic displacements at those stations have little contributions to the summation while the number of stations, that is, denominator of eq. (7), increases. However, the values are still quite different from the theoretical ones if we include only 54 or 103 stations, which are within 40° or 50° distances from the epicentre. The values are (−68.5, 0.8, −149.9) for the former and (−39.0, 0.9, −82.1) for the latter, respectively, for the three components of the rotation vector.

For the Tohoku-Oki earthquake, however, the magnitudes of rotation were much larger than the theoretical values and the directions of rotation were opposite. There were many geodetic stations distributed near the epicentre, but they were in the western side of the epicentre. The lack of any station on the eastern side of the epicentre destroys the orthogonal property of the spherical harmonics, as shown in the summation in eq. (7). In this way, the contributions from co-seismic displacements of all degrees except degree one and from spheroidal co-seismic displacements are not cancelled out. As a result, it is the asymmetry of the station distribution in the near-field that causes large rotation magnitudes and opposite directions of rotation. This shows that the co-seismic displacements of high degrees and of spheroidal ones are aliased in the observed rotation parameters.

Not similarly to the Sumatra earthquake, the co-seismic displacements within 10° distance in which 42 stations are included dominate the summation in eq. (7). However, the rotation vector determined by these 42 stations is much larger than the theoretical ones. Including more stations with larger epicentric distance just increases the number of stations and then decreases the rotation vector, as Fig. 5(d) shows.

The results computed by transformation method are also quite different from the theoretical ones (see Table 2). If we only use part of the stations, for example, near-field stations, the differences will be larger. These larger differences show that due to poor network configuration transform method cannot provide reliable rotation parameters. Since the rotation parameters are related to the horizontal displacements, if we set vertical displacements at the geodetic stations to be zeroes, the results will be (6.4, 3.8, 8.8) and (189.7, 266.7, −78.2) for Sumatra and Tohoku-Oki earthquakes, respectively. They differ a little from the situation that the vertical displacements are taken into account. This means the horizontal displacement dominate the rotation parameters when using transformation method.

3.4 Uncertainty of uncorrected co-seismic effect on rotation

Measured coordinate time series have known or unknown offsets. Uncorrected offsets have a detrimental impact on velocity estimation. Currently, the co-seismic offsets in coordinate time series are identified and removed by either manual or automated approaches. Gazeaux *et al.* (2013) made an experiment on detecting the offsets using simulated data by different methods. Their results showed that manual methods almost always give better results than automated or semi-automated methods and the smallest magnitude of offset detectable by manual method is 5 mm. However the offsets caused by small or far-field earthquakes may not be detected by manual method due to their smaller magnitudes although the occurrence times are accurately known.

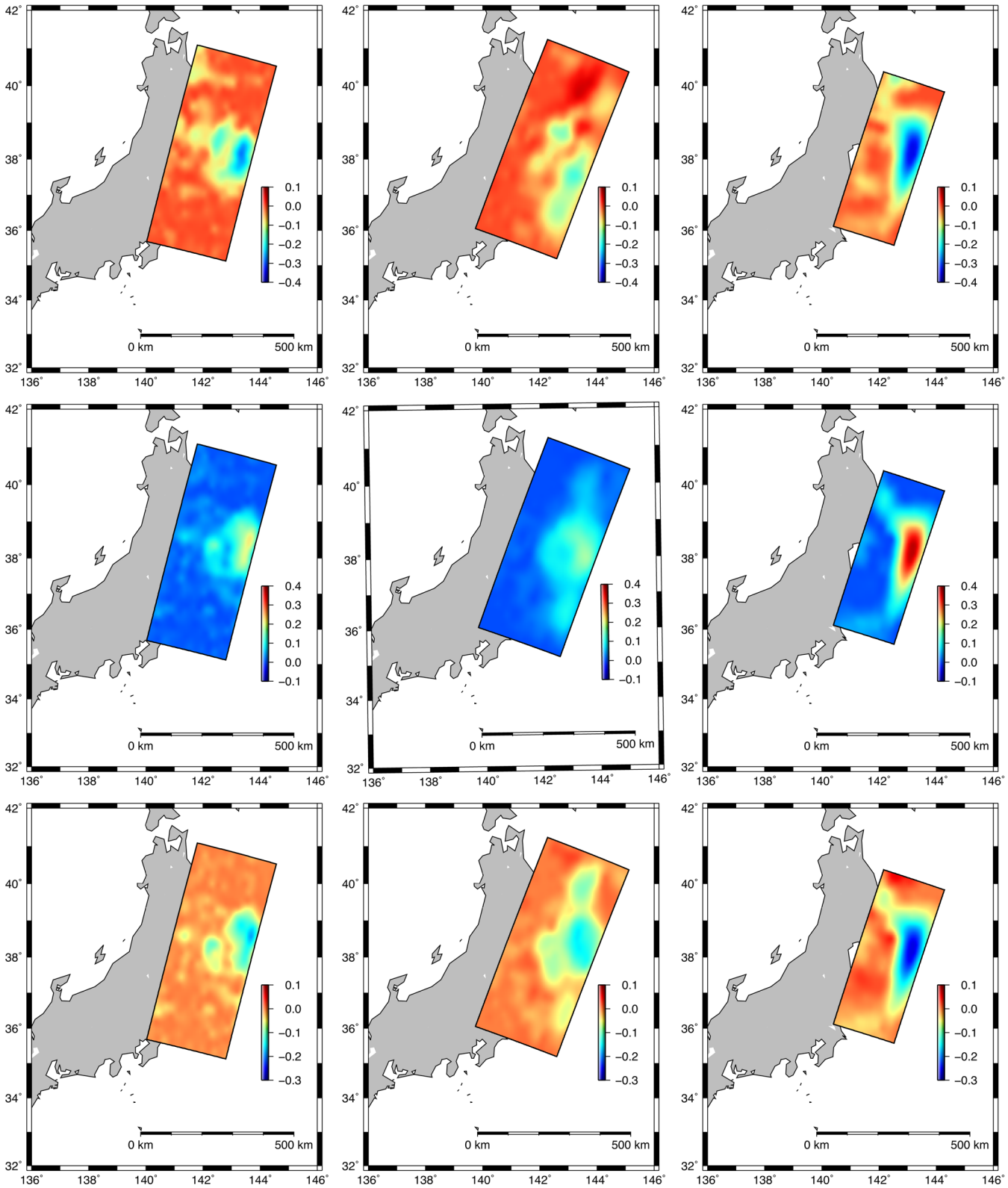

Figure 4. The same as Fig. 2, but for the 2011 Tohoku-Oki earthquake.

Specifically, the cumulative effect of these small offsets is non-negligible and the manual method inevitably induces man-made uncertainties.

To see to what extent the uncorrected co-seismic displacements affect the rotation, we first set a threshold value. Among the 937 stations, when the co-seismic offsets are smaller than the threshold, we consider the offsets can't be found and remain in the coordinates; when the offsets are larger than the threshold, we consider the offsets are corrected but with Gaussian uncertainties due to manual processing. Then we set the variance of the Gaussian uncertainties

Table 2. Theoretical and observed earthquake-induced CF frame rotation parameters.

	2004 Sumatra earthquake	2011 Tohoku-Oki earthquake
Moment (10^{22} N m)	3.95	5.31
Fault geometry (°) Rake/strike/dip	110.0/329.0/8.0	88.0/203.0/10.0
*R*x (μas)	−19.5 (−2.4/5.6)	−68.4 (136.8/187.1)
*R*y (μas)	−6.2 (−0.1/3.9)	67.4 (−353.6/263.6)
*R*z (μas)	−51.5 (−11.6/8.8)	−48.8 (424.7/−78.7)
$\|\boldsymbol{R}\|$ (μas)	55.4 (11.8/11.5)	107.7 (449.4/336.5)

Note: Values in parentheses are computed according to eq. (7)/eq. (10).

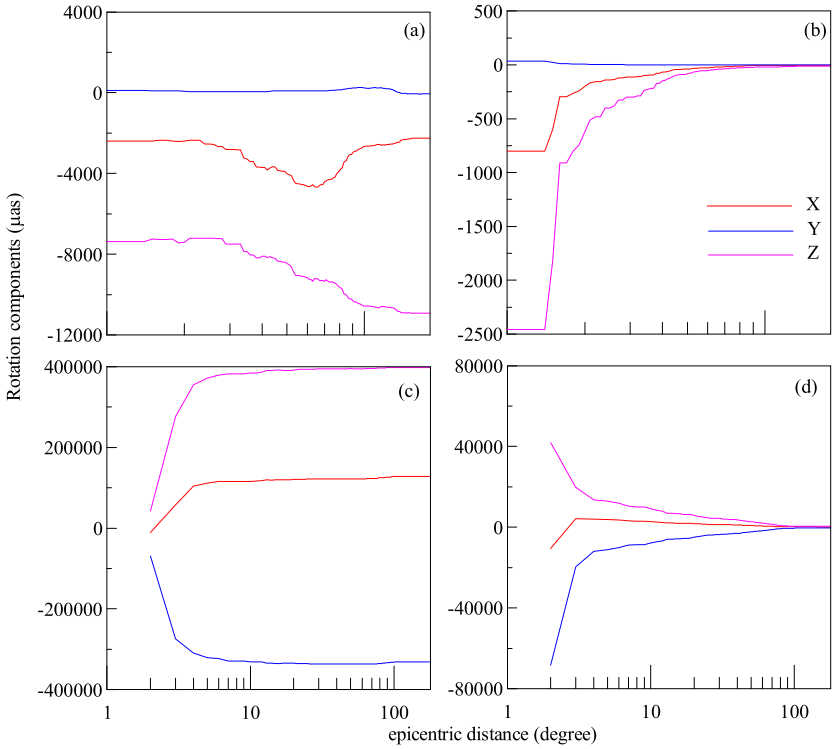

Figure 5. Variations of three rotation components with respect to the epicentric distance. (a) and (b) are the summation and the rotation (summation divided by station number), respectively, for the 2004 Sumatra earthquake; (c) and (d) are similar to (a) and (b) correspondingly, but for the 2011 Tohoku-Oki earthquake.

Table 3. Evaluation of the uncertainty of the uncorrected co-seismic effect.

	2004 Sumatra earthquake			2011 Tohoku-Oki earthquake		
Threshold (mm)	0.1	0.5	1.0	0.1	0.5	1.0
Variance (mm)	0.1	0.5	1.0	0.1	0.5	1.0
*R*x (μas)	− 1.02 ± 0.02	− 1.92 ± 0.05	− 1.20 ± 0.06	− 0.13 ± 0.03	− 2.65 ± 0.10	− 4.60 ± 0.10
*R*y (μas)	0.16 ± 0.02	0.04 ± 0.03	0.29 ± 0.03	− 0.24 ± 0.03	− 3.26 ± 0.09	− 3.28 ± 0.10
*R*z (μas)	− 0.21 ± 0.02	0.80 ± 0.04	0.61 ± 0.06	− 1.00 ± 0.03	− 3.82 ± 0.07	− 5.11 ± 0.07

identical to the threshold value and produce white noises. And finally we applied transformation method to compute rotation due to unidentified co-seismic offsets and white noise. To achieve reliable statistical results, we totally compute 10 000 times. Some statistical results are listed in Table 3.

For the Sumatra earthquake, the uncorrected co-seismic effect does not increase obviously with the threshold because the geodetic stations are far away from the epicentre such that the co-seismic displacements at those stations are mainly smaller than the threshold. Therefore increasing threshold affects little on the rotation. This may explain why the stations which are less affected can be used to construct reference frame as Tregoning *et al.* (2013) proposed. On the contrary for the Tohoku-Oki earthquake, the larger threshold causes heavier uncorrected co-seismic effect on rotation since there are many near-field stations. For example, when the threshold is 1.0 mm which is the positioning precision required in terrestrial reference frame, the effect on rotation has a magnitude of 7.6 μas which corresponds to about 0.2 mm. Therefore, the co-seismic displacements at the stations near the epicentre need more attention to be identified and removed. Tregoning *et al.* (2013) confirmed the considerable effect of small and uncorrected co-seismic deformation on site velocity and hence the plate rotation. It is shown that CF frame is also affected by small and uncorrected co-seismic deformation.

4 CONCLUSIONS

A method to estimating the rotation change in the orientation of the CF frame attributable to earthquakes involving the point dislocation theory based on a SNERI Earth model is here introduced. Rotation change in the orientation is related solely to the co-seismic toroidal displacements of degree one on the Earth's surface and independent of the spheroidal displacements and of other degrees. Therefore it is here concluded that the spheroidal deformation of the Earth due to other dynamic processes, such as surface loading, does not rotate the CF frame. However, in practice, this will be highly distorted by the network effect when we use finite geodetic stations.

Among the four types of independent dislocation types, that is, vertical strike-slip, vertical dip slip, horizontally and vertically tensile ones, only the vertical dip slip dislocation produced any toroidal displacement of degree one. In this way, it was the only type that caused the CF frame to rotate. As a consequence, the large and reverse earthquake that occurs in the subduction zone is likely to change the orientation of the CF frame.

We modified the toroidal displacement solution of degree one by introducing the stratified density distribution, and the numerical values were computed using the PREM model. Then the values were used on the two recent large earthquakes. The results showed that the Sumatra and Tohoku-Oki earthquakes both caused the CF frame to rotate by at least tens of μas. Using the approximated value of 1.465×10^{-15} for toroidal displacement on the Earth's surface is valid, which makes the computation simpler.

The CF frame is of great importance to geodesy and it plays a critical role in the realization of the international terrestrial reference system. For these reasons, changes in the CF frame due to Earth's deformation should be taken into account in precise geodesy and its use. More attention was paid to the origin change of CF frame before. Meanwhile the rotation change of CF frame deserves to be studied from now on. However, properly observing the earthquake-induced rotation of the CF frame demands a good configuration of the geodetic network. Specifically, the lack of near-field stations around the epicentre may cause the smaller rotation magnitude and the uneven or asymmetric distribution of the stations destroys the orthogonal property of the spherical harmonics, distorting the results devastatingly. Our simple summation method and the transformation method are difficult to detect the rotation of CF frame caused by two recent large earthquakes using displacement observations at the tracking stations. Therefore an improved method is expected. As a result, evaluating earthquake-induced CF frame rotation by the present geodetic network requires more considerations.

ACKNOWLEDGEMENTS

We are grateful to Shuhei Okubo and an anonymous reviewer for their helpful and constructive comments that greatly improved the manuscript. This study was financially supported by the '973' project (Grant No. 2014CB845902) and the National Natural Science Foundation of China projects (Grant Nos 41374025 and 41321063). The second author was financially supported by the National Natural Science Foundation of China (Grant Nos 41474059, 41331066 and 41174063) and by the Chinese Academy of Science/State Administration of Foreign Experts Affairs international partnership program for creative research teams (No. KZZD-EW-TZ-19), as well as the State Key Laboratory of Geodesy and Earth's Dynamics foundation (SKLGED2014-1-1-E). The third author was financially supported by the National Natural Science Foundation of China (Grant Nos 11173050 and 11373059).

REFERENCES

Altamimi, Z., Collilieux, X. & Metivier, L., 2011. ITRF2008: an improved solution of the international terrestrial reference frame, *J. Geod.,* **85,** 457–473.

Ben-Menahem, A. & Singh, S.J., 1968. Eigenvector expansions of Green's dyads with applications to geophysical theory, *Geophys. J. R. Astron. Soc.,* **16,** 417–452.

Blewitt, G., 2003. Self-consistency in reference frames, geocenter definition, and surface loading of the solid Earth, *J. geophys. Res.,* **108**(B2), doi:10.1029/2002JB002082.

Chen, J.L., Wilson, C.R., Eanes, R.J. & Nerem, R.S., 1999. Geophysical interpretation of observed geocenter variations, *J. geophys. Res.,* **104,** 2683–2690.

Chlieh, M. *et al.*, 2007. Coseismic slip and afterslip of the Great Mw 9.15 Sumatra-Andaman Earthquake of 2004, *Bull. seismol. Soc. Am.,* **97**(1A), S152–S173.

Collilieux, X., Altamimi, Z., Coulot, D., van Dam, T. & Ray, J., 2010. Impact of loading effects on determination of the International Terrestrial Reference Frame, *Adv. Space Res.,* **45,** 144–154.

Dong, D., Dickey, J.O., Chao, Y. & Cheng, M.K., 1997. Geocenter variations caused by atmosphere, ocean and surface groundwater, *Geophys. Res. Lett.,* **24**(15), 1867–1870.

Dong, D., Qu, W., Fang, P. & Peng, D., 2014. Non-linearity of geocentre motion and its impact on the origin of the terrestrial reference frame, *Geophys. J. Int.,* **198,** 1071–1080.

Dong, D., Yunck, T. & Heflin, M., 2003. Origin of the International Terrestrial Reference Frame, *J. geophys. Res.,* **108**(B4), 2200, doi:10.1029/2002JB002035.

Dziewonski, A.M. & Anderson, D.L., 1981. Preliminary reference earth model, *Phys. Earth planet. Inter.,* **25,** 297–356.

Gazeaux, J. *et al.*, 2013. Detecting offsets in GPS time series: first results from the detection of offsets in GPS experiment, *J. geophys. Res.,* **118,** 2397–2407.

Han, S.C., Shum, C.K., Bevis, M., Ji, C. & Kuo, C.Y., 2006. Crustal dilatation observed by GRACE after the 2004 Sumatra-Andaman earthquake, *Science,* **313,** 658–662.

Hayes, G., 2011. Finite fault model: updated result of the March 11, 2011 Mw 9.0 earthquake offshore Honshu, Japan, report, Earthquake Hazards Program, U.S. Geol. Surv., Reston, VA. Available at: http://earthquake.usgs.gov/earthquakes/world/japan/031111_M9.0_prelim_geodetic_slip.php.

IERS Conventions, 2010. IERS Technical Note No. 36, eds Petit, G. & Luzum, B., Frankfurt am Main: Verlag des Bundesamts für Kartographie und Geodäsie, 179 pp.

Ji, C., 2004. Available at: http://neic.usgs.gov/neis/eq_depot/2004/eq_041226/result/static_out.

Jin, S.G. & Park, P.H., 2006. Strain accumulation in South Korea inferred from GPS measurements, *Earth Planets Space,* **58**(5), 529–534.

Jin, S.G., Zhang, L. & Tapley, B.D., 2011. The understanding of length-of-day variations from satellite gravity and laser ranging measurements, *Geophys. J. Int.,* **184**(2), 651–660.

Jin, S.G., van Dam, T. & Wdowinski, S., 2013. Observing and understanding the Earth system variations from space geodesy, *J. Geodyn.,* **72,** 1–10.

Métivier, L., Greff-Lefftz, M. & Altamimi, Z., 2010. On secular geocenter motion: the impact of climate changes, *Earth planet. Sci. Lett.,* **296,** 360–366.

Okubo, S., 1993. Reciprocity theorem to compute the static deformation due to a point dislocation buried in a spherically symmetric earth, *Geophys. J. Int.,* **115,** 921–928.

Shao, G., Li, X., Ji, C. & Maeda, T., 2011. Focal mechanism and slip history of 2011 Mw 9.1 off the Pacific coast of Tohoku earthquake, constrained with teleseismic body and surface waves, *Earth Planets Space,* **63**(7), 559–564.

Sun, W., 1992. Potential and gravity changes raised by dislocations in spherically symmetric earth models, *PhD thesis*, The University of Tokyo, Japan.

Sun, W. & Dong, J., 2014. Geo-center movement caused by huge earthquakes, *J. Geodyn.,* **76,** 1–7.

Sun, W. & Okubo, S., 1993. Surface potential and gravity changes due to internal dislocations in a spherical earth – I. Theory for a point dislocation, *Geophys. J. Int.,* **114,** 569–592.

Sun, W. & Okubo, S., 1998. Surface potential and gravity changes due to internal dislocations in a spherical Earth, II: Application to a finite fault, *Geophys. J. Int.,* **132,** 79–88.

Sun, W., Okubo, S. & Vaníček, P., 1996. Global displacements caused by point dislocations in a realistic Earth model, *J. geophys. Res.,* **101**(B4), 8561–8577.

Takeuchi, H. & Saito, M., 1972. Seismic surface waves, *Methods Comput. Phys.,* **11,** 217–295.

Tregoning, P., Burgette, R., McClusky, S.C., Lejeune, S., Watson, C.S. & McQueen, H., 2013. A decade of horizontal deformation from great earthquakes, *J. geophys. Res.,* **118,** 2371–2381.

Wei, S., Sladen, A. & the ARIA group, 2011. Updated result 3/11/2011 (Mw 9.0), Tohoku-oki, Japan, report. Calif. Inst. of Technol., Pasadena. Available at: http://www.tectonics.caltech.edu/slip_history/2011_taiheiyo-oki/.

Wu, X., Ray, J. & van Dam, T., 2012. Geocenter motion and its geodetic and geophysical implications, *J. Geodyn.,* **58,** 44–61.

Zhang, X.G. & Jin, S.G., 2014. Uncertainties and effects on geocenter motion estimation from global GPS observations, *Adv. Space Res.,* **54**(1), 59–71.

Zhou, J., Sun, W.K., Sun, H.P. & Xu, J.Q., 2013. Reformulation of co-seismic polar motion excitation and low degree gravity changes: applied to the 2011 Tohoku-Oki earthquake (M_w9.0), *J. Geodyn.,* **63,** 20–26.

Zhou, J., Sun, W. & Dong, J., 2015. A correction to the article "Geo-center movement caused by huge earthquakes" by Wenke Sun and Jie Dong, *J. Geodyn.,* **87,** 67–73.

APPENDIX A: TOROIDAL DISPLACEMENTS OF DEGREE ONE

The differential equations for solving the toroidal deformation of the Earth are as follows (Takeuchi & Saito 1972; Sun *et al.* 1996):

$$\left.\begin{aligned}\frac{\mathrm{d}y_{1,t}}{\mathrm{d}r} &= \frac{1}{r}y_{1,t} + \frac{1}{\mu}y_{2,t}\\ \frac{\mathrm{d}y_{2,t}}{\mathrm{d}r} &= -\frac{3}{r}y_{2,t}\end{aligned}\right\}. \tag{A1}$$

Here, the conditions at core-mantle boundary ($r = a_c$) and on the Earth's surface are as follows:

$$y_{2,t}(a_c) = y_{2,t}(a) = 0. \tag{A2}$$

According to the second equality of eqs (A1) and (A2) and condition that $y_{2,t}$ is continuous [according to the zero source function of $y_{2,t}$ (Okubo 1993)], one can derive that $y_{2,t}$ is always zero. Then the first equality of eq. (A1) produces the following:

$$\left.\begin{aligned}y_{1,t}(r) &= c_1 r, \quad r_s < r \le a\\ y_{1,t}(r) &= c_2 r, \quad a_c \le r < r_s\\ y_{1,t}(r) &= 0, \quad r < a_c\end{aligned}\right\} \tag{A3}$$

The two unknown parameters of c_1 and c_2 are to be determined and r_s is the hypocentre location. The source condition of $y_{1,t}$ (discontinuity across the hypocentre) is as follows (Okubo 1993; Sun *et al.* 1996):

$$c_1 - c_2 = \frac{s_1^t}{r_s} = \frac{3}{16\pi r_s^3}. \tag{A4}$$

Another condition for determining c_1 and c_2 stems from eq. (2) in Section 2:

$$c_1\,[f(a) - f(r_s)] + c_2\,[f(r_s) - f(a_c)] = 0, \tag{A5}$$

where

$$f(r) = \int_0^r \rho r^4 \mathrm{d}r. \tag{A6}$$

This can be computed by adopting the Earth model. Finally, the toroidal horizontal displacement of degree one is as follows:

$$y_{1,t}(r) = \frac{3a}{16\pi r_s^3}\frac{f(r_s) - f(a_c)}{f(a) - f(a_c)}. \tag{A7}$$